International Journal of Innovative Research and Advanced Studies (IJIRAS)
Volume 7 Issue 5, May 2020

ISSN: 2394-4404

Report On Best Locations For Deploying Large-Scale Photovoltaics And Photovoltaic Systems

Oluwasola O. Ademulegun

College of Engineering, Swansea University, Bay Campus, Swansea, UK

Michael O. Kolawole

Jolade Strategic Environmental & Engineering Consultants, Moorabbin East Victoria, Australia

Abstract: ***A photovoltaic (PV) system, a renewable energy system, generates electricity from the Sun. While the performance of the PV is dependent on some environmental conditions and their component configurations, it is interesting to know how the performance of PVs varies in relation to other geographical locations. In this paper, a comparative study is undertaken to look at the relative performance of PVs deployed in 200 country areas of distinct geography and climate, using the Solargis and the National Aeronautics and Space Administration databases: the key attributes being average temperature, irradiance, landmass, and population density. The environmental factors affecting any PV – irradiance and temperature – are reviewed, verified with simulation, and results are validated with laboratory experiments. By modelling extrapolation, the PV performances figures for many countries based on landmass, population density, average irradiation and average temperatures are obtained, scaled and plotted for comparison and analysis. Fifty-four high-performance areas were identified which were further sub-divided into three groups: the classification is done according to the potential performance ranks of the locations. The results further suggest the areas where the PV could be deployed for better relative performance for large-scale energy generation from PV.***

Keywords: Deploying large-scale photovoltaic; Locational photovoltaic performances; Photovoltaic characteristics; Relative photovoltaic performance; Solar energy

I. INTRODUCTION

The increasing concerns of global warming arising from the emission of greenhouse gases have made the probing into alternative ways of generating energy especially necessary. The use of renewable energy systems, like photovoltaic (PV) and wind energy systems, offers opportunities for achieving significant reductions in greenhouse gas emissions. PV systems generate electricity from the Sun. *PV cells* are made of various s*emiconductors* that have ability to experience the movement of electrons within their structure when exposed to the visible light and infrared rays. The PV cells can be configured into modules and arrays to convert the energy of the Sun to supply safe and clean solar energy in appreciable quantities. A review of the design, operation and maintenance of PV systems is given in (Hernandez-Callejo et al., 2019). Two environmental conditions that influence actual efficiency are solar irradiance (radiant energy from the Sun) and temperature (of module and/or of air). A method of analysing global energy potential has been proposed in (Korfiati et al., 2016). Another methodology that groups the world into 12 regions and classifies PV performances based on the climate of the regions using temperature, precipitation, and irradiation has been presented in (Ascencio-Vasquez et al., 2019). A review of the previous estimates of PV potentials, with emphasis on technical and sustainability limits, has been given in (Castro et al., 2013).

The behaviour of the PV under varying climatic conditions is well researched. However, an understanding of the potential of the PV at different geographical locations of national boundaries could help in large-scale deployment of PV systems. Several questions come to light: if a PV system were to be set up at some places on the earth's surface, where should that system be set up for optimum advantage – basing the decision on the geography around and the science of photovoltaics? How does setting up that PV system at one

ISSN: 2394-4404

location compare to setting up the system in some other places? How do space factors – the availability of land and population density – affect the potentials of PV project at a location in comparison with most other locations? These are the questions this paper aims to answer.

In the subsequent sections, we show how the differences in the geographic features of locations comparatively impact the performance plus deployment feasibility of photovoltaics – done with quantification and data aggregation for clear comparison. A study of the locational characteristic performance of a PV is important to understanding the relative benefit of the PV at different locations and helps in identifying comparative advantages. The knowledge could help in effective installation of large-scale solar power generating systems using long-distance transmission for large-scale redistribution of renewable energy.

II. AN OVERVIEW OF PHOTOVOLTAICS AND PHOTOVOLTAIC SYSTEMS

Photovoltaics is the process of directly converting light into electricity at the atomic level, and on materials (for example, semiconductors) that exhibit photoelectric property – effect that causes them to absorb photons of light and release electrons (NASA, 2019). By capturing these free electrons, electricity is generated. The semiconductors are made into solar cells, which are in turn made into solar panels. A PV system makes use of solar panels to intercept the light from the Sun to generate direct current (dc) electricity. When the solar cells are electrically connected to each other and mounted in a support structure or frame, they are called a photovoltaic module or photovoltaic panel. Multiple modules/panels can be wired together to form an array, Figure 1. The modules are mounted on free space–rooftops, open field, and wall, where they can receive solar radiation without obstruction. Sometimes the modules are set on trackers to follow the radiation of the Sun through the day.

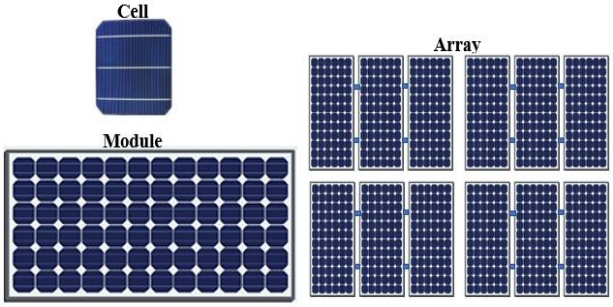

Figure 1: Photovoltaic Cell, Module, and Array

To date, there are three types of solar cells, namely; monocrystalline solar cell, polycrystalline solar cell, and amorphous solar cells, of which monocrystalline solar cells and polycrystalline solar cells are the most common and most efficient (Taşçioğlu et al., 2016). The efficiency at which PV cells convert sunlight to electricity varies by the type of semiconductor material and PV cell technology. A typical silicon cell could be about 100-200 cm^2. Research studies are on-going towards achieving PVs of higher efficiencies.

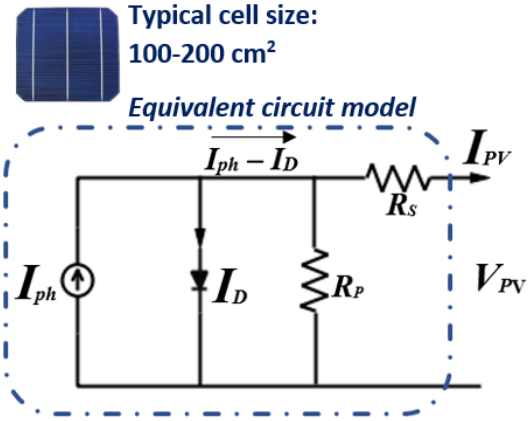

Figure 2: Equivalent Circuit of Photovoltaic Cell

Figure 2 depicts the equivalent circuit of a typical solar cell that consists of a current source and a diode in parallel, with series and shunt resistances (Zhou and Macaulay, 2017). As a precaution, when cells are joined in series, shading one cell could cause a destruction of the shaded cell or the lamination material causing the PV module to burst. The partial shading effect could be avoided by connecting bypass diodes across cells to prevent large voltage differences in the reverse-current direction within the solar cells. Usually, one bypass diode is connected across every 15 to 20 cells. The bypass diodes also prevent an abrupt drop in voltage and power during any event of partial shading (Ahmed et al., 2017). Figure 3 depicts a typical arrangement of bypass diodes around modules.

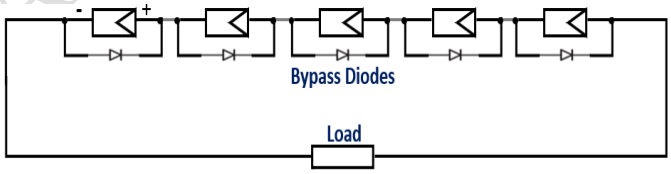

Figure 3: Parallel Cells with Bypass Diodes

A. EFFECTS OF TEMPERATURE AND IRRADIANCE ON PV PERFORMANCE

Performance evaluation of PV systems depends on cells' arrangement and positioning (that is, optimum exposure to the sun, no overshadowing), module temperature, and reference cell selected in measuring the irradiance in the plane of the array (POA). Suppose these constraints are observed, the PVs properties and behaviour under various operating conditions could be examined by simulation using the equivalent PV cells circuit of Figure 2. The simulations are carried out using the MATLAB Simulink library tools. The I-V and P-V electrical output characteristics of the PV are observed under operating conditions of irradiance and temperature. From the equivalent circuit model of Figure 2, output current

$$I_{PV} = a_k(I_{Ph} - I_D), \quad (1)$$

where

$$a_k = \frac{R_P}{R_P + R_S}$$

If the effects of the shunt and series resistances in Figure 2 are negligible, that is, $R_p \gg R_s$, then $a_k \approx 1$. From basic circuit theory, suppose we have three cell resistances R_{p1}, R_{p2}, and R_{p3} with values 120 Ω, 130 Ω, and 140 Ω, respectively

(semiconductors have unique internal characteristics) that are connected in parallel – their equivalent resistance R_{pt} = 0.923 Ω ≈ 1 Ω. So, with cells configured in parallel, a_k is constant boosting output current I_{PV}.

$$I_{PV} = N_p(I_{Ph} - I_D) \quad (2)$$

and the *Diode Current*, $I_D = I_0\left[\left(e^{\frac{qV_D}{nkN_ST_C}}\right) - 1\right]$ (3)

With the equivalent sum of series and parallel resistances advisedly taken as constant at 1 – having one cell in parallel and having $R_p \gg R_s$; the current and the voltage generated by the PV are modelled with the following equations (Cubas et al., 2014) and (Nakagawa et al., 2016).

Photo-generated Current,

$$I_{Ph} = \left(I_{SC} + C_t\,(T_C - T_{ref})\right).\frac{S}{S_{ref}} \quad (4)$$

$$\text{For} \quad I_0 = I_{RS}\left(\frac{T_C}{T_{ref}}\right)^3.exp\left[\frac{qE_g}{nk}\left(\frac{1}{T_{ref}} - \frac{1}{T_C}\right)\right],$$

$$I_{RS} = \frac{1}{exp\left(\frac{qV_{OC}}{N_SnkT_C}\right)-1}\,I_{SC} \quad (5)$$

In Figure 2 and in Eq. (1) to Eq. (5), the notations used and the other parameters of the PV are defined: a_k = *equivalent cell resistance =1,* I_{ph} *= photo-generated current in PV cell (A),* I_D *= diode current (A),* I_0 *= saturation current at reference temperature = 1.2 * 10*$^{-7}$ *A, q = electric charge = 1.60 * 10*$^{-19}$ *C,* V_D *= diode voltage (V), n = ideality factor = 1.54, k = Boltzmann constant = 1.38 * 10*$^{-23}$ *J/K,* N_p *= number of cells in parallel in module = 1,* N_s *= number of cells in series in module = 36,* T_c *= actual cell temperature (K),* I_{sc} *= short circuit current at reference conditions/cell = 2 A,* C_t *= temperature coefficient of photon current = 1.7 * 10*$^{-3}$ *A/K,* T_{ref} *= reference cell temperature = 298 K (25*^{o}*C),* S_{ref} *= reference irradiance = 1000 W/m*^{2}*, S = actual irradiance (W/m*^{2}*),* I_{RS} *= cell reverse saturation current (A),* I_{PV} *= PV output current (A),* E_g *= band gap energy of semiconductor = 1.103 eV,* R_s *= series resistance of PV cell (Ω),* R_P *= parallel resistance of PV cell (Ω),* V_{PV} *= voltage of PV cell (V).*

For a PV module having 36 cells, with each cell having an area of 0.0069 m^2, if the maximum voltage is denoted by V_{max}(V) and the maximum current is denoted by I_{max}(A).

$$Module\ area = 36 \times 0.0069 \approx 0.25\ m^2$$

$$Efficiency\ of\ PV\ module = \frac{V_{max}\,I_{max}}{Irradiance \times Module\ area\ (m^2)} \times 100\% \quad (6)$$

The effects of changing irradiance on the I-V and P-V characteristics, short circuit current (I_{sc}) and open circuit voltage (V_{oc}) at a constant temperature are observed. Similarly, the effects of temperature variations at constant irradiance are observed. The behaviour of the PV module when partially shaded is mimicked with simulation using interconnection of three modules, one operating under normal conditions and the other two having different irradiances, one with parallel diode and the other without a parallel diode.

B. EXPERIMENTAL VERIFICATION OF EFFECTS OF TEMPERATURE AND IRRADIANCE

The essential characteristics of the PV panel, in harnessing the energy of the Sun, are further verified for real PV panel using a PV Simulator and an Electronic Load Unit (ELU) system that regulates the PV's terminal voltage and absorbs power, Figure 4. The ELU has meters that measure the panel's output voltage, power, and current, and the Lamp plays the role of the Sun; supplying the panel with irradiance in the form of illumination as well as serving as a source of heat to raise the temperature of panel.

At 25^{o}C temperature and at 1000 W/m^2 irradiance level; the open circuit voltage of the PV panel is 23 V, and the short circuit current is 2 A. Three panels are connected in series and then in parallel to see the results of the different panel interconnections. The laboratory experiment includes thermal meter for temperature measurement. The PV characteristics are then considered in a globe-wide comparative locational performance assessment for PVs.

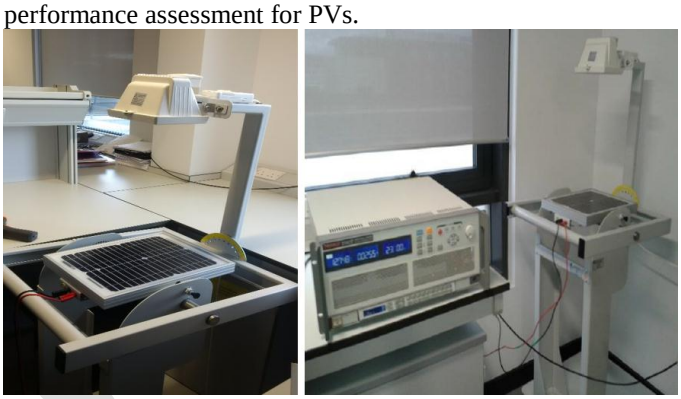

(a) The Lamp of the Electronic Load Unit *(b) Electronic Load Unit System*

Figure 4: Experimental Setup for PV Characteristics Verification

C. GLOBE-WIDE PV PERFORMANCE ASSESSMENT

The metrics used in determining the performance of the PV and the defining locational characteristics of national boundaries are described in the following sections.

a. KEY PERFORMANCE PARAMETERS

The average irradiance and the average temperature – the key factors affecting any PV performance – are measured for each location. With the key factors affecting the power output of the PV determined, its ability to harness the energy of the Sun at the different locations could be ascertained. The global irradiance and average-temperature measurements are drawn respectively from databases of Solargis (Solargis, 2019) and the National Aeronautics and Space Administration (NASA, 2019), Table 1 in the Appendix.

The distribution of irradiation is quantified by scaling each level of irradiation of a country over the entire landmass of the country; as an example, suppose a country's irradiation distribution is given in Figure 5, irradiation levels (in kWh/m^2) 5.8, 6.2, and 6.6 represent the leading irradiations – these will have weighted values of 2.5, 1.25, and 1.25 respectively – on a weighting scale of 5. The country area then has a weighted average Global Horizontal Irradiance (GHI) value of 10.17.

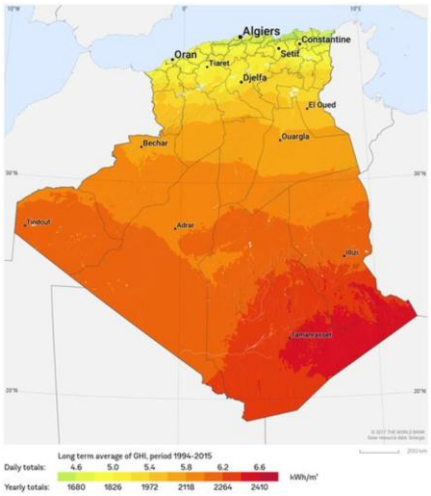

Figure 5: A Sample Map of Global Horizontal Irradiance (GHI)

The GHI has been used rather than say the Direct Normal Irradiance (DNI) or the Diffuse Horizontal Irradiance (DHI) because GHI – which combines both DNI and DHI – gives the best representation of the position of a real PV installation with respect to the Sun, compare to either DNI or DHI. For GHI, the solar incident ray strikes the planar surface of the PV at an angle. Using either DNI or DHI could, perhaps, lead to the same result as using GHI at most locations but not without slight differences at some locations of geographical particularities (Ruiz-Arias, Jose A.; Gueymard, 2018), (Jacobson, Mark Z.; Jadhav, 2018), and (Gueymard, A. Christian; Ruiz-Arias, 2016).

The GHI data for Sweden and Norway were not available; having the two country's locations (latitude, longitude), populations, neighbouring countries' GHIs, and landmass data, an estimate of their status is made. The mean of temperatures in January, June, and December are taken as the country-wide mean annual temperature. The landmass and population data of each country area are used in estimating population density in persons/km^2 – data obtained given in Table 1 in the Appendix.

b. GROUPING COUNTRY AREAS

Using each location's characteristics and the verified performance characteristics of a PV, a globe-wide comparative locational performance assessment for the PV is done. Areas with similar performances are grouped together in order. With the fundamental characteristics of the PV established such that the variation in the performance of the PV with irradiances and temperatures is determined, and taking into cognizance the availability of land area and the population density; an analyses of the potential performance of PVs in 200 national boundaries – comprising countries and islands – is performed. The analysis is carried out for each of the national boundaries.

As noted from the introduction, an attempt is being made to ascertain those optimal locations where solar PVs could be deployed for relatively higher performances based on area's irradiance, temperature, landmass, and population density as key metrics. While the work seeks to identify the areas of better relative PV performances, the work is not claiming that the PV will not have reasonable output power in the other areas of less relative performances. Including the landmass and population density in the performance metrics reveals the locations where large-scale PV systems could naturally be deployed with comparative advantages.

The average GHI is given as

$$GHI = \left(\frac{10}{W_1} \times GHI_1\right) + \left(\frac{10}{W_2} \times GHI_2\right) + \left(\frac{10}{W_3} \times GHI_3\right), \quad (7)$$

Where GHI_1, GHI_2, and GHI_3 are the three most predominant GHIs over country land area; W_1, W_2, and W_3 are scaling factors used in weighing GHI levels. The average temperature, T_{av} is calculated as

$$T_{AV} = \left(\frac{25}{m_1} \times T_1\right) + \left(\frac{25}{m_2} \times T_2\right) + \left(\frac{25}{m_3} \times T_3\right), \quad (8)$$

where T_1, T_2, and T_3 are three measures of temperature for country over a year; m_1, m_2, and m_3 are scaling factors. The national boundaries are then grouped according to:

GROUP A:

- ✓ *Average GHI* ≥ 9
- ✓ *Mean annual temperature* $\langle T_{av} \rangle < 29^o C$
- ✓ *Land area > 25 (km^2 per 400,000)*
- ✓ *Population density < 4.6 (Persons/km^2 per 15)*

GROUP B:

- ✓ $8 \leq$ *Average GHI* ≤ 11
- ✓ *Mean annual temperature* $\langle T_{av} \rangle < 31^o C$
- ✓ *1 < Land area < 23 (km^2 per 400,000)*
- ✓ *Population density < 7.4 (Persons/km^2 per 15)*

GROUP C:

- ✓ $7 \leq$ *Average GHI* ≤ 10
- ✓ *Mean annual temperature* $\langle T_{av} \rangle < 27^o C$
- ✓ *0.7 < Land area < 24 (km^2 per 400,000)*
- ✓ *Population density < 31 (Persons/km^2 per 15)*

III. RESULTS AND DISCUSSION

The subsequent sections present the results of the simulation, the laboratory experiment, and a discussion of the globe-wide locational performance of the PV. That a PV produces more power when irradiance is higher and when temperature is lower is already established. The simulation and the laboratory experiments have been performed to verify and validate the established behaviour of the PV – this, in addition to the other locational metrics, serves as the basis for comparing the performance of the PV at the different national boundaries of distinct average irradiances and temperatures.

A. RESULT OF CHARACTERISTIC PERFORMANCE OF PV FROM SIMULATION

The essential property of any PV panels gives an indication of how panels perform under various environmental conditions that could serve as input factors to the PV panels. Tables 2 and 3, with the associated Figures 6 and 7, indicate that, higher irradiance leads to increase in current, I_{sc}, and voltage, V_o. For example, from Table 2, when the irradiance is at 1000 W/m^2; I_{sc}, V_{oc}, V_{max} and I_{max} are 2.0090 A, 23.38 V, 19.66 V and 1.8862 A, respectively. When the irradiance is at 600 W/m^2; I_{sc}, V_{oc}, V_{max} and I_{max} are 1.2050 A, 22.66 V, 18.98 V and 1.1175 A, respectively.

When the irradiance is even lower at 200 W/m^2; I_{sc}, V_{oc}, V_{max} and I_{max} fall further to 0.4017 A, 21.12 V, 17.48 V and 0.3713 A, respectively. This follows from the theory of operation of semiconductors in that the higher incident rays cause more movement of electrons within the semiconductor, making more current to flow in an opposite direction to the movement of the electrons. Meanwhile, an increase in temperature leads to a decrease in output voltage and less output power. From Table 2, when the temperature is at 25^{o}C the maximum output power of the module is 35.64 W. However, as the temperature increases to 75^{o}C, the output power falls to 22.16 W.

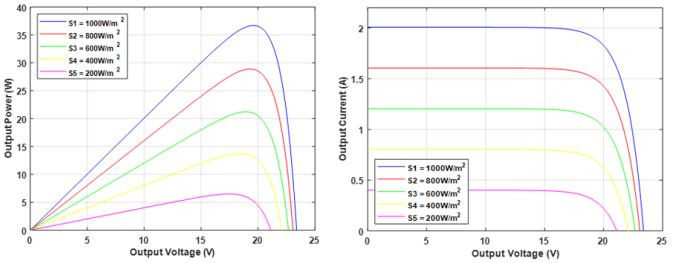

(a) Plot of PV output power against voltage (b) Plot of PV output current against voltage

Figure 6: Photovoltaic Performance with Irradiance at Constant Temperature (25^{o}C)

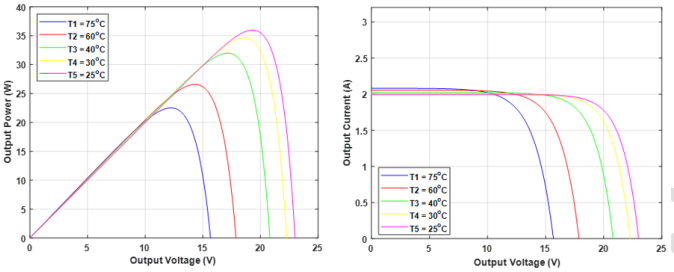

(a) Plot of PV output power against voltage (b) Plot of PV output current against voltage

Figure 7: Photovoltaic Performance with Temperature at Constant Irradiance (1000 W/m^2)

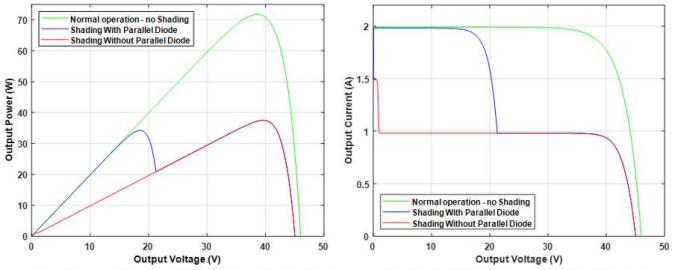

(a) Plot of PV output power against voltage (b) Plot of PV current against Voltage

Figure 8: Plots of Photovoltaic Characteristic Performances during Shading

Irradiance (W/m^2)	I_{SC} *(A)*	V_{OC} *(V)*	V_{max} *(V)*	I_{max} *(A)*	P_{max} *(W)*	*Efficiency (%)*
1000	2.0090	23.38	19.66	1.8862	36.69	14.77
800	1.6070	23.06	19.38	1.4902	28.88	14.53
600	1.2050	22.66	18.98	1.1175	21.21	14.23
400	0.8034	22.08	18.52	0.7403	13.71	13.80
200	0.4017	21.12	17.48	0.3713	6.49	13.06

Table 2: Variation in Irradiance at Constant Temperature, (25^{o}C)

Temperature (ºC)	I_{SC} *(A)*	V_{OC} *(V)*	V_{max} *(V)*	I_{max} *(A)*	P_{max} *(W)*	*Efficiency (%)*
75	2.085	15.63	12.12	1.8283	22.16	8.92
60	2.059	17.85	14.26	1.8394	26.23	10.56
40	2.026	20.80	17.11	1.8486	31.63	12.73
30	2.009	22.26	18.52	1.8526	34.31	13.81
25	2.000	22.99	19.16	1.8601	35.64	14.35

Table 3: Variation of Temperature at Constant Irradiance, (1000 W/m^2)

B. RESULT OF CHARACTERISTIC PERFORMANCE OF PV FROM LAB EXPERIMENT

The results from the experimental method confirms the results of the Simulink modelling – comparing Table 2 with Table 4, Table 3 with Table 5, Figure 6 with Figure 9, and Figure 7 with Figure 10.

Irradiance (W/m^2) Regulated using the slide switch	I_{sc} *(A)*	V_{oc} *(V)*	V_{max} *(V)*	I_{max} *(A)*	P_{max} *(W)*	*Efficiency (%)*
Zero irradiance (panel covered)	0.0310	1.030			0	0
Room light irradiance	0.0351	15.291	12.494	0.0317	0.40	5.8
Lamp slide switch "ON" at middle position	0.1317	20.242	18.296	0.1222	2.24	12.98
Lamp slide switch "ON" at top position	0.1935	20.473	18.598	0.1803	3.35	13.87

Table 4: Irradiance Characteristics (Experimental Method)

Temperature (^{0}C) Regulated using the "ON" Time of Lamp	*Temperature (^{O}C)*	I_{sc} *(A)*	V_{oc} *(V)*	V_{max} *(V)*	I_{max} *(A)*	P_{max} *(W)*
Room light condition	27.3	0.210	20.80	17.37	0.186	3.23
Lamp turned "ON" in first few seconds	28.5	0.222	20.40	17.67	0.202	3.57
Lamp "ON" (3 minutes)	35.6	0.226	19.92	17.42	0.203	3.54
Lamp "ON" (6 minutes)	41.3	0.227	19.61	17.11	0.201	3.44
Lamp "ON" (10 minutes)	45.9	0.228	19.30	16.36	0.206	3.37

Table 5: Temperature Characteristics (Experimental Method)

Connecting PV modules together in series, or in parallel, leads to a higher output power, Figure 11 - compare with Figure 9(a), with respect to output power. The P-V curves indicate a possible point to which a PV could be set to operate to achieve maximum power output – using a maximum power point tracking technique.

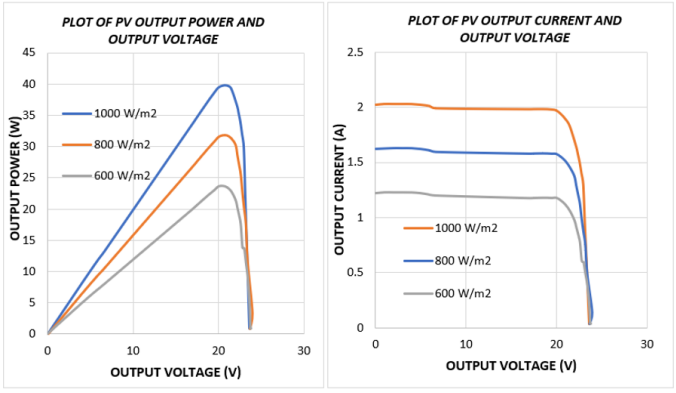

(a) Plot of module power against voltage (b) Plot of module current against voltage

Figure 9: Module Characteristics with Irradiance at Constant Temperature

ISSN: 2394-4404

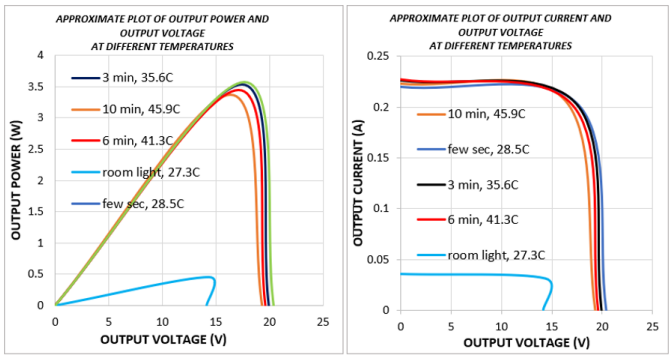

(a) Plot of module power against voltage (b) Plot of module power against voltage

Figure 10: Module Characteristics with Temperature at Constant Irradiance

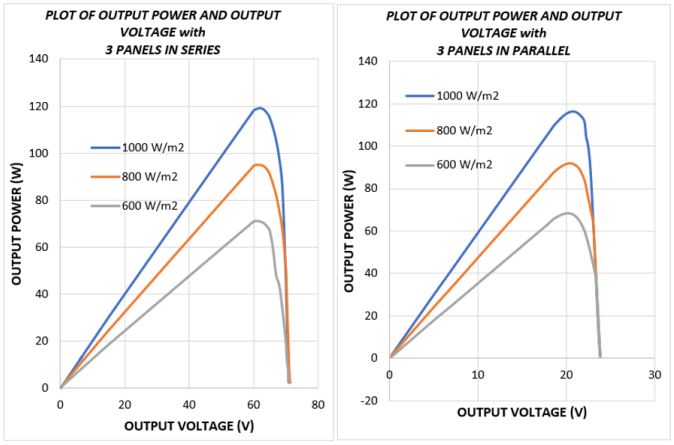

(a) Three modules connected in series (b) Three modules connected in parallel

Figure 11: Output power of Interconnection of Modules

There is a drastic drop in current when partial shading occurs in the PV lacking a parallel diode, Figure 8. While the partial shading incidence reduces the overall performance of the PV system, an inclusion of a parallel diode prevents abrupt drop in PV output power – suggesting that; in setting up modules, to avoid the partial shading effects, it is important to locate modules where there is little or no likelihood of shading, usually on plain or desert-like lands, or on top of structures that are away from obstructions. The results confirm the report on the behaviour of a PV module under varying conditions of temperature and irradiance given in (Ahmed et al., 2017) and (Cubas et al., 2014).

C. GLOBE-WIDE LOCATIONAL PERFORMANCE OF PV

The efficiency of the PV module increases with increasing level of irradiance and at lower temperatures. The observed PV characteristics indicate that PV modules have better chances of producing more output power during the day and at locations of higher solar irradiances and/or lower temperatures, verified in the sections 3.1 and 3.2. The observed PV behaviour form the foundation of the globe-wide comparative locational performance assessment of PV.

Of the 200 national boundaries analysed, 54 country areas have appreciable performances. The 54 areas are further grouped according to the level of performance; Group-A being the countries with the best performances, Group-B locations being the second in rank, and followed by Group-C locations, in that order. For each of the groups, a plot of average GHI – land area – population density and a plot of average temperature – land area – population density is created. For comparison of performances and clarity of plots, the land area has been unitised in km^2 per 400,000 while the population density has been unitised in persons per km^2 per 15.

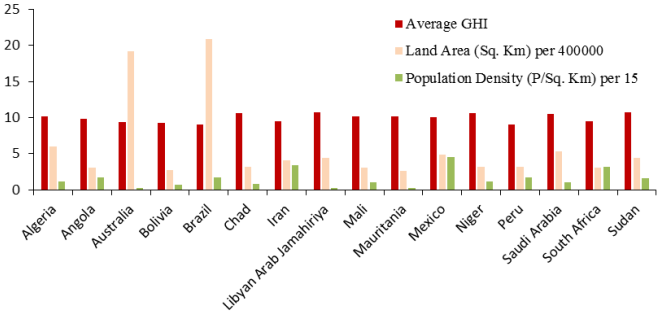

Figure 12: Irradiance – Land Area – Population Density of Countries in Group-A

Based on the performance metrics – irradiance, temperature, land area, and population density; the countries in Group-A – the best performance group – are Algeria, Angola, Australia, Bolivia, Brazil, Chad, Iran, Libyan Arab Jamahiriya, Mali, Mauritania, Mexico, Niger, Peru, Saudi Arabia, South Africa, and Sudan – Figures 12 and 13; followed by countries in Group-B – second-rank performance group – which are Afghanistan, Botswana, Chile, Colombia, Egypt, Ethiopia, Kenya, Madagascar, Mongolia, Mozambique, Namibia, Republic of Yemen, Somalia, South Sudan, Tanzania, USA, Venezuela, and Zambia – Figures 14 and 15; followed by countries in Group-C – the final rank group – which are Cameroon, China, Cote d'Ivoire, DR Congo, India, Indonesia, Iraq, Kazakhstan, Malaysia, Morocco, Myanmar, Nigeria, Oman, Pakistan, Spain, Thailand, Turkey, Turkmenistan, Uzbekistan, and Zimbabwe – Figures 16 and 17.

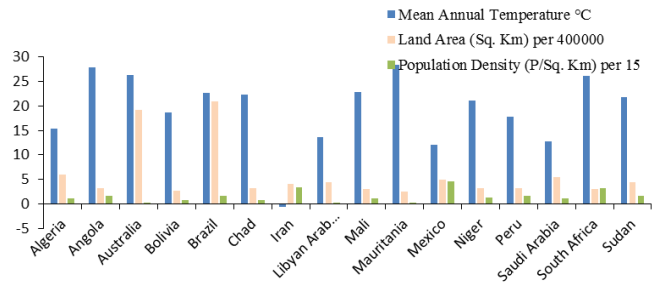

Figure 13: Temperature – Land Area – Population Density of Countries in Group-A

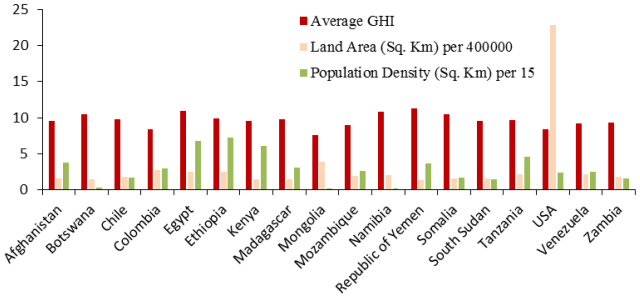

Figure 14: Irradiance – Land Area – Population Density of Countries in Group-B

ISSN: 2394-4404

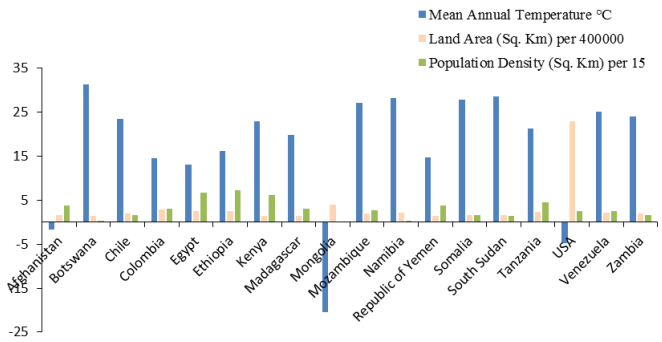

Figure 15: Temperature – Land Area – Population Density of Countries in Group-B

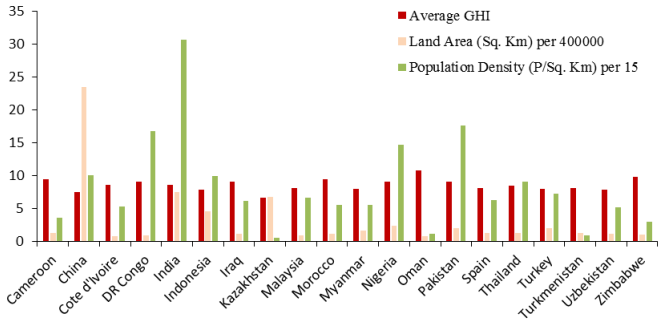

Figure 16: Irradiance – Land Area – Population Density of Countries in Group-C

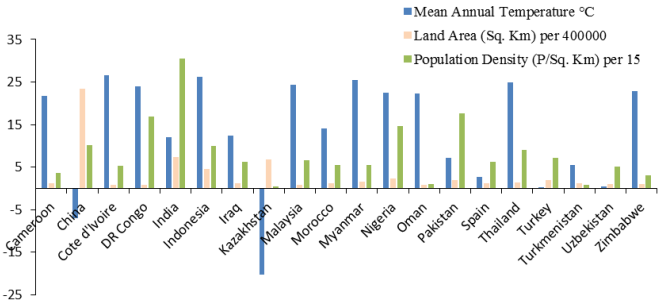

Figure 17: Temperature – Land Area – Population Density of Countries in Group-C

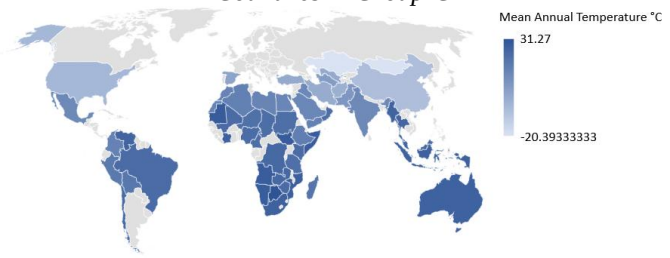

Figure 18: Globe-wide Mean Annual Temperature of Countries

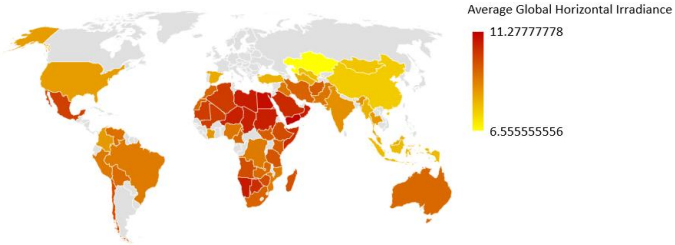

Figure 19: Globe-wide Relative Global Horizontal Irradiance of Countries

Figure 20: Globe-wide Relative Population Density of Countries

Comparative maps – that show the relative figures of temperatures, irradiances and population densities – for the 54 best PV-performance areas indicate the relative potentials of PVs, Figures 18, 19, and 20. The parameters have been normalised for each land area so that the values remain uniform through each of the national boundaries. It could be noted that larger part of Africa, Australia, and parts of Latin America have favourable irradiance levels. Some other national boundaries have less irradiance but favourable lower temperatures which makes the PV perform considerable. Some areas are relatively less populated, which could naturally signify much more space for large-scale PV installations, especially countries with desert-lands, like Algeria, Angola, Australia, Bolivia, Chad, Egypt, Iran, Libyan Arab Jamahiriya, Mali, Mauritania, Niger, Peru, Saudi Arabia, and Sudan.

IV. CONCLUSIONS

The science of the characteristics of photovoltaics serves as the foundation for analysing how the performance of a photovoltaic system could vary with location. Taking the characteristic of any photovoltaic, with the landmass and the population information of 200 national boundary locations, the performance of deployed photovoltaic system at different locations is comparable. Doing the performance analysis using the Solargis and the NASA databases, with temperature, irradiance, landmass, and population density as the key input metrics; 54 national boundary locations have appreciable performances. When the locations are sub-grouped based on performance, locations in most part of Africa, Australia, and parts of Latin America are among high-performance areas. Some locations with lower irradiance still rank high because of favourable lower temperatures and/or larger landmass and/or lower population densities. Some high-performance locations in the Sahara Desert, Asia, and Australia added another advantage: they are desert-lands for un-obstructed space for deployment of large-scale photovoltaic systems.

REFERENCES

[1] Ahmed, J., Salam, Z., Lung, Y., Kashem, S. (2017). A Fast MPPT Technique Based on I-V Curve Characteristics Under Partial Shading 1696–1701.

[2] Ascencio-Vasquez, Julian; Brecl, Kristijan; Topic, M. (2019). Methodology of Köppen-Geiger-Photovoltaic climate classification and implications to worldwide mapping of PV system performance. Sol. Energy 191,

672–685. https://doi.org/https://doi.org/10.1016/j.solener.2019.08.072
[3] Castro, C. De, Mediavilla, M., Javier, L., Frechoso, F. (2013). Global solar electric potential : A review of their technical and sustainable limits. Renew. Sustain. Energy Rev. 28, 824–835. https://doi.org/10.1016/j.rser.2013.08.040
[4] Cubas, J., Pindado, S., Manuel, C. De, Universitario, I., Ignacio, D.M., Riva, D., Upm, I.D.R. (2014). Parameters Based on Analytical Formulation and the 4098–4115. https://doi.org/10.3390/en7074098
[5] Gueymard, A. Christian; Ruiz-Arias, J.A. (2016). Extensive worldwide validation and climate sensitivity analysis of direct irradiance predictions from 1-min global irradiance. Sol. Energy 128, 1–30. https://doi.org/https://doi.org/10.1016/j.solener.2015.10.010
[6] Hernandez-Callejo, Luis; Gallardo-Saavedra, Sara; Alonso-Gomez, V. (2019). A review of photovoltaic systems: Design, operation and maintenance. Sol. Energy 188, 1–15. https://doi.org/https://doi.org/10.1016/j.solener.2019.06.017
[7] Jacobson, Mark Z.; Jadhav, V. (2018). World estimates of PV optimal tilt angles and ratios of sunlight incident upon tilted and tracked PV panels relative to horizontal panels. Sol. Energy 169. https://doi.org/https://doi.org/10.1016/j.solener.2018.04.030
[8] Korfiati, Athina; Gkonos, Charalampos; Veronesi, Fabio; Gaki, Ariadni; Grassi, Stefano; Schenkel, Roland; Volkwein, Stephan; Raubal, Martin; Hurni, L. (2016). Estimation of the Global Solar Energy Potential and Photovoltaic Costwith the use of Open Data. Int. J. Sustain. Energy Plan. Manag. 09, 17–30.
[9] Nakagawa, K., Tanaka, T., Suzuki, T. (2016). Modelling of Photovoltaic Module Using Matlab Simulink Modelling of Photovoltaic Module Using Matlab Simulink 2–11. https://doi.org/10.1088/1757-899X/114/1/012137
[10] NASA. (2019). POWER Data Access Viewer Prediction Of Worldwide Energy Resource [WWW Document]. URL https://power.larc.nasa.gov/data-access-viewer/
[11] NASA (2019). What is Photovoltaics? [WWW Document]. URL https://science.nasa.gov/science-news/science-at-nasa/2002/solarcells (accessed 9.27.19).
[12] Ruiz-Arias, Jose A.; Gueymard, A.C. (2018). Worldwide inter-comparison of clear-sky solar radiation models: Consensus-based review of direct and global irradiance components simulated at the earth surface. Sol. Energy 1–20. https://doi.org/https://doi.org/10.1016/j.solener.2018.02.008
[13] Solargis (2019). Solar resource maps and GIS data for 200+ countries [WWW Document]. URL https://solargis.com/maps-and-gis-data/overview
[14] Taşçioğlu, A., Taşkin, O., Vardar, A. (2016). A Power Case Study for Monocrystalline and Polycrystalline Solar Panels in Bursa City, Turkey. Int. J. Photoenergy 2016. https://doi.org/10.1155/2016/7324138
[15] Zhou, Z., Macaulay, J. (2017). An emulated PV source based on an unilluminated solar panel and DC power supply. Energies 10. https://doi.org/10.3390/en10122075

APPENDIX I

Country	Average Temperature (°C)	Weighted Average GHI (kWh/m^2)	Land Area (km^2)	Population Density (Person/km^2)	Population Density (P/km^2)/15
Afghanistan	-1.66	9.53	652860	56.66	3.78
Albania	3.48	6.74	27400	107.20	7.15
Algeria	15.37	10.17	2381740	17.84	1.19
Andorra	5.86	0.00	470	163.92	10.93
Angola	27.88	9.85	1246700	25.28	1.69
Antigua and Barbuda	27.10	9.56	440	235.94	15.73
Argentina	23.91	9.20	2736690	16.44	1.10
Armenia	-3.86	6.93	28470	103.13	6.88
Aruba	27.54		180	588.62	39.24
Australia	26.36	9.36	7682300	3.25	0.22
Austria	2.18	5.15	82409	106.33	7.09
Azerbaijan	9.02	6.97	82658	120.87	8.06
Bahamas	24.92	9.13	10010	40.17	2.68
Bahrain	18.19		760	2130.25	142.02
Bangladesh	14.96	7.87	130170	1287.69	85.85
Barbados	27.28		430	667.09	44.47
Belarus	-3.85	5.02	202910	46.52	3.10
Belgium	4.94	4.97	30280	381.30	25.42
Belize	26.12	8.50	22810	17.02	1.13
Benin	25.71	8.92	112760	103.92	6.93
Bolivia	18.59	9.26	1083300	10.46	0.70
Bosnia and Herzegovina	3.38	6.79	51000	68.67	4.58
Botswana	31.27	10.43	566730	4.17	0.28
Brazil	22.72	9.00	8358140	25.36	1.69
British Virgin Islands	27.08		150	213.85	14.26
Brunei Darussalam	27.26		5270	83.10	5.54
Bulgaria	2.41	6.42	108560	64.49	4.30
Burkina Faso	22.46	9.83	273600	73.72	4.91
Burundi	18.95	8.83	25680	447.06	29.80
Cambodia	27.08	8.74	176520	93.02	6.20
Cameroon	21.82	9.36	472710	53.19	3.55
Canada	-17.55	4.88	9093510	4.09	0.27
Cape Verde	23.38		4030	138.59	9.24
Cayman Islands	27.18		240	262.18	17.48
Central African Republic	23.27	9.56	622980	7.71	0.51
Chad	22.34	10.67	1259200	12.46	0.83
Chile	23.42	9.79	743532	24.61	1.64
China	-7.10	7.50	9388211	151.12	10.07
Colombia	14.46	8.44	1109500	44.84	2.99
Congo	23.95	8.20	341500	251.85	16.79
Cook Islands		9.47	240	72.70	4.85
Costa Rica	20.85	8.13	51060	97.67	6.51
Cote d'Ivoire	26.60	8.50	318000	79.77	5.32
Croatia	6.08	6.32	55960	74.10	4.94
Cuba	24.78	9.39	106440	107.96	7.20

Table 1: Average temperature, weighted irradiance, and population density of national boundaries